FOSSEE, IIT Bombay
OpenFOAM Case Study Project
June 2024

Dynamics of Porous Cylinders

Jonathan Thomas John[1] and Chandan Bose[2]

[1]Department of Mechanical Engineering, Indian Institute of Technology (Indian School of Mines), Dhanbad
[2]Assistant Professor, Aerospace Engineering, College of Engineering and Physical Sciences, The University of Birmingham

July 25, 2024

Synopsis

Steady flow through and around porous cylinders was modeled in OpenFOAM and studied numerically. Porosity was modeled using the Darcy-Forchheimer equation and implemented in OpenFOAM with the pisoFoam solver. The drag coefficient, wake geometry, velocity and pressure gradients were studied and verified with previously published literature on porous cylinders. Compared to solid cylinders, it was observed that porous cylinders have a lower drag coefficient, longer wake and unlike solid cylinders, the wake penetrates into the cylinder region. Additionally, a solid cylinder with a porous coating was modeled and the results were compared with those of solid and fully porous cylinders.

1 Introduction

A porous medium is one which is not completely solid, consisting of voids through which fluid may pass. In the context of Fluid Dynamics, a porous medium has a behavior that may be seen is 'in-between' an impervious medium, which allows no fluid to pass through, and a cavity, which allows fluid to pass through freely. The study of porous media is relevant to problems involving particle transport, filtration and pollutant management, etc. Porous coating on bluff bodies has been observed to modify the flow physics significantly, which may provide novel solutions in field such as aerodynamics, structural design etc.

Laminar flow around a circular cylinder is an extensively covered topic in the domain of fluid dynamics and is well documented using experimental as well as computational techniques. It is an important and challenging problem to tackle as it exhibits the phenomena of boundary layer separation, wake formation as well as vortex shedding, which are relevant in broader fields of engineering and fluid dynamics such as structural design, aeroacoustics etc. This problem has been studied over a range of flow regimes (distinguished by Reynolds number) by Rajani et al. [1] who documented how parameters such as drag and lift coefficients vary with the different flow regimes in 2D laminar as well as 3D turbulent cases.

Steady flow around and through a permeable circular cylinder has been studied by Yu et al. [2] over a range of Darcy numbers and Reynolds numbers. Streamlines, velocity profiles, wake geometry and critical Reynolds number for the onset of recirculating wakes were examined for different Darcy numbers. An interesting phenomenon was observed in the laminar regime where the recirculating wake was detached from the cylinder, in contrast to solid cylinders where the recirculating wake forms at the surface of the cylinder.

2 Governing Equations and Models

2.1 Problem definition

To implement the permeability equation (Darcy-Forchheimer equation) in OpenFOAM and model the steady dynamics of completely porous and porous-coated cylinders and compare the results with those of completely impervious cylinders, with respect to drag coefficient and wake geometry.

2.2 Governing equations

The incompressibility equation and Navier-Stokes equation for two dimensional, steady, laminar flow of an incompressible, viscous fluid in the homogeneous fluid region, in the vector form is given as:

$$\nabla \cdot \vec{u} = 0 \tag{1}$$

$$\nabla \cdot (\rho \vec{u}\vec{u}) = -\nabla p + \mu \nabla^2 \vec{u} \tag{2}$$

As elaborated by Yu et al. [2], the porous medium is considered to be rigid, homogeneous, isotropic, and saturated with the same single-phase fluid as that in the homogeneous fluid region. The governing equations for the porous region, based on the Darcy-Brinkman-Forchheimer extended model, are given as:

$$\nabla \cdot \vec{u} = 0 \tag{3}$$

$$\nabla \cdot \frac{(\rho \vec{u}\vec{u})}{\varepsilon} = -\nabla(\varepsilon p*) + \mu \nabla^2 \vec{u} - \frac{\mu \varepsilon}{K}\vec{u} - \frac{\rho \varepsilon C_f |\vec{u}|}{\sqrt{K}}\vec{u} \tag{4}$$

where, $\vec{u}$ is the local average velocity vector (Darcy velocity), $p*$ is the intrinsic average pressure, μ is the dynamic viscosity of the fluid, ε is the porosity of the porous medium, K is the permeability, and $C_f = 1.75/\sqrt{150\varepsilon^3}$ is the Forchheimer coefficient. The left hand side is the convective term and the terms on the right hand side, are the pressure term, Brinkman term, Darcy term and Forchheimer term respectively.

The non-dimensional parameters relevant to this study are:

- Reynolds number, $Re = \frac{\rho U d}{\mu}$, where ρ is the density of the fluid, U is the inlet velocity, d is the diameter of the cylinder and μ is the dynamic viscosity of the fluid.
- Darcy number, $Da = \frac{K}{d^2}$, where K is the permeability of the porous medium given by $K = \frac{1}{D}$, where D is the Darcy coefficient in the Darcy-Forchheimer equation.

- Coefficient of drag, C_d which is obtained from drag force, $F_d = \frac{1}{2} C_d \rho A U^2$, where A is the reference area which is unity for a cylinder of unit diameter.

2.3 Geometry and Mesh

The meshes for all three cases were made using the open source finite-element mesh generation software Gmsh and implemented in OpenFOAM using the gmshToFoam command.

The main geometry structure used for the three cases consists of four blocks surrounding the cylinder of unit diameter and one block downstream to observe the wake, as shown in Figure 1. Although the cases are 2D, the entire geometry is extruded by unit length in the perpendicular direction as OpenFOAM only supports 3D geometries.

For the fully porous case, a square of side 1.414 is added inside of the main cylinder, creating five more blocks to facilitate mesh refinement inside the cylinder, as shown in Figure 3.

For the annular porous coated case, the solid cylinder is of diameter 0.5 and is positioned concentrically within the larger cylindrical region to produce a solid cylinder with an annular porous coating, as shown in Figure 4.

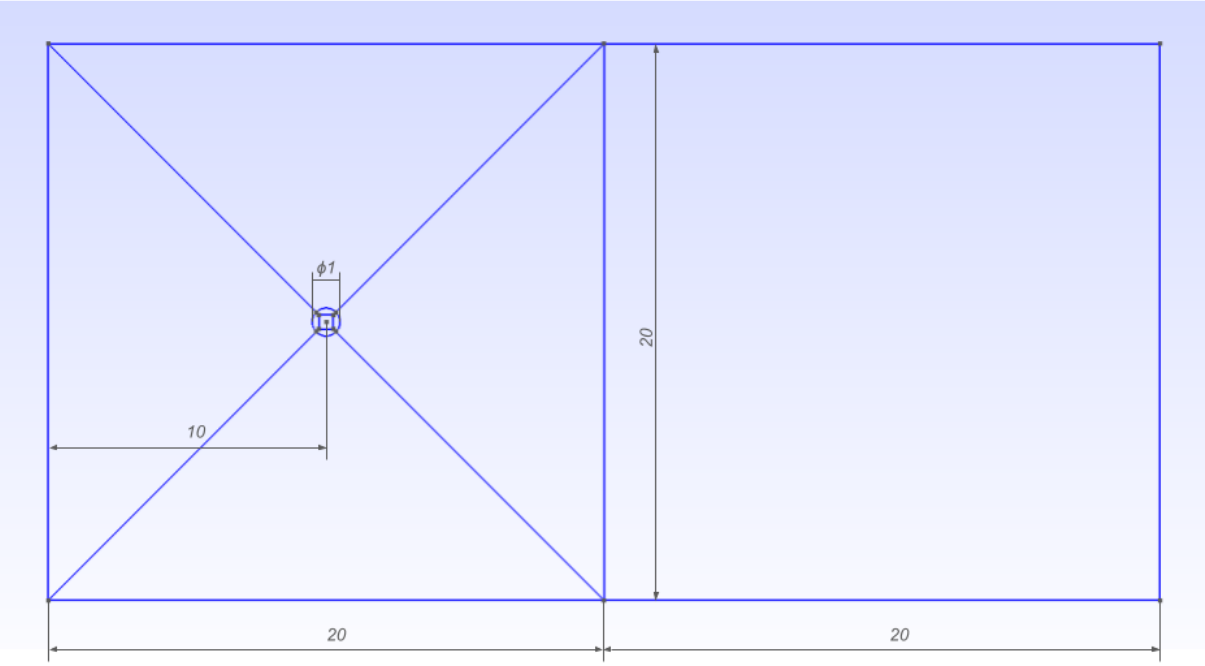

Figure 1: Computational Domain

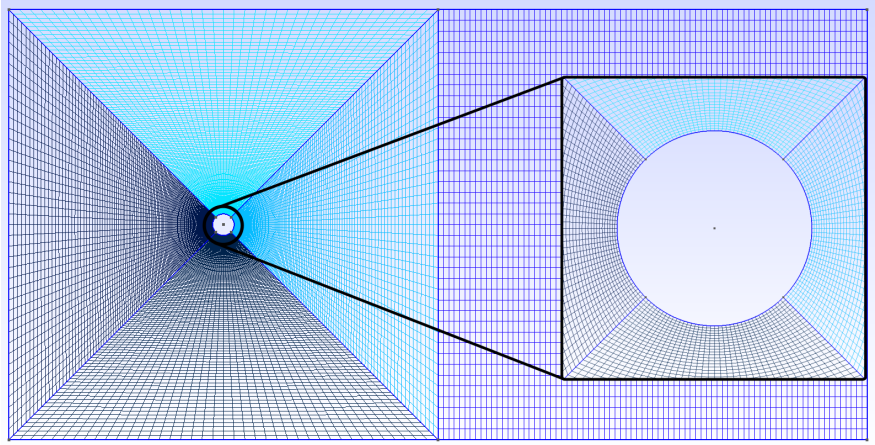

Figure 2: Mesh for Solid Cylinder

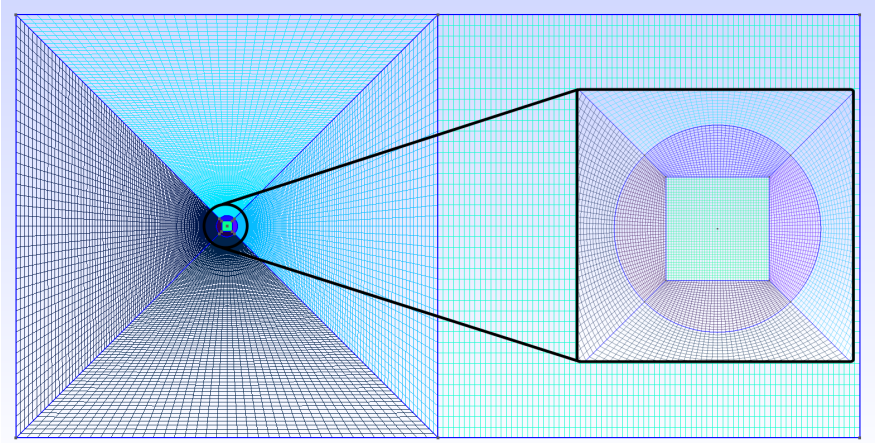

Figure 3: Mesh for Fully Porous Cylinder

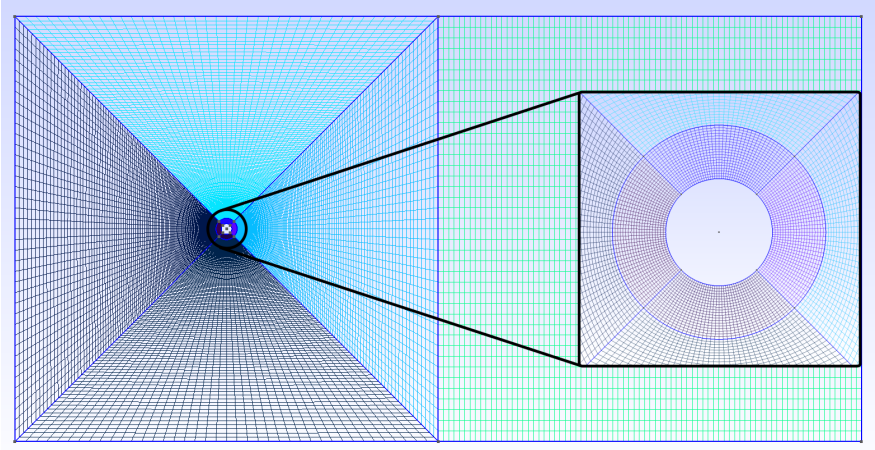

Figure 4: Mesh for Porous Coated Cylinder

2.4 Boundary Conditions

The boundary conditions were set as shown to obtain a standard case for flow around a cylinder:

Patch Name	**Condition Type**	**Value** (ms^-1)
inlet	fixedValue	(1 0 0)
outlet	zeroGradient	-
walls	slip	-
cylinder *(only in fully porous and solid cases)*	fixedValue	(0 0 0)
outerCylinder *(only in porous coated case)*	fixedValue	(0 0 0)
innerCylinder *(only in porous coated case)*	fixedValue	(0 0 0)

Table 1: Velocity (U) Boundary Conditions

Patch Name	**Condition Type**	**Value** (m^2s^-2)
inlet	zeroGradient	-
outlet	fixedValue	0
walls	zeroGradient	-
cylinder *(only in fully porous and solid cases)*	zeroGradient	-
outerCylinder *(only in porous coated case)*	zeroGradient	-
innerCylinder *(only in porous coated case)*	zeroGradient	-

Table 2: Kinematic Pressure (p) Boundary Conditions

It is important to note that the parameter 'p' defined in OpenFOAM is not pressure but rather kinematic pressure, which is defined as pressure divided by fluid density.

2.5 Solver setup

2.5.1 pisoFoam

The solver used is pisoFoam, which is a pressure-based solver designed for transient simulations of incompressible flow. pisoFoam implements the PISO (Pressure-Implicit with Splitting of Operators) algorithm for pressure-momentum coupling. This solver was chosen as it supports porosity and can solve steady as well as transient cases.

The PISO algorithm can be summarised as follows:

1. Set the boundary conditions.
2. Solve the discretised momentum equation to compute an intermediate velocity field.
3. Compute the mass fluxes at the cells faces.
4. Solve the pressure equation.
5. Correct the mass fluxes at the cell faces.
6. Correct the velocities on the basis of the new pressure field.
7. Update the boundary conditions.
8. Repeat from 3 for the prescribed number of times.
9. Increase the time step and repeat from 1.

Steps 4 and 5 can be repeated to correct for non-orthogonality.

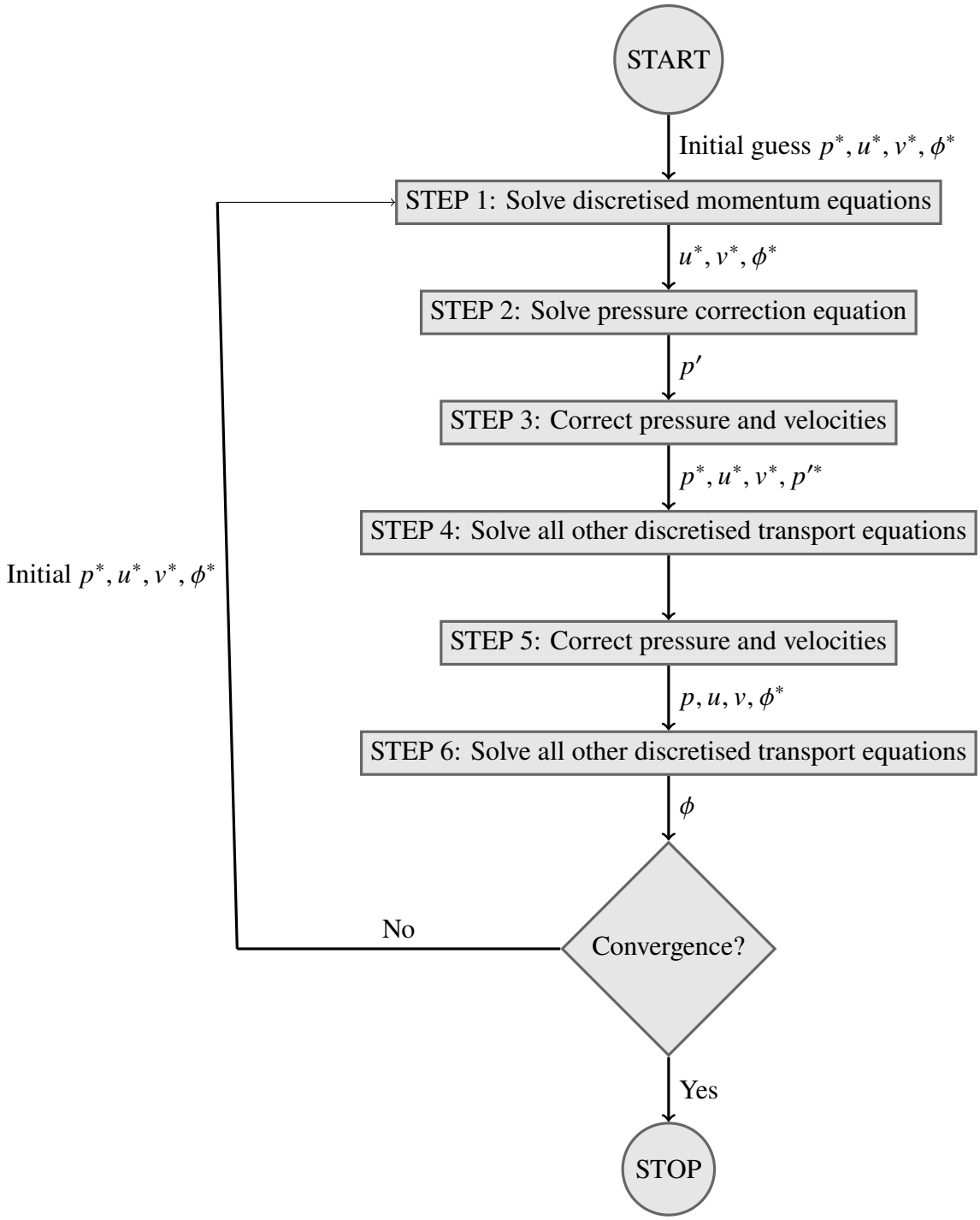
START
Initial guess p^*, u^*, v^*, ϕ^*
STEP 1: Solve discretised momentum equations
u^*, v^*, ϕ^*
STEP 2: Solve pressure correction equation
p'
STEP 3: Correct pressure and velocities
p^*, u^*, v^*, p'^*
STEP 4: Solve all other discretised transport equations
Initial p^*, u^*, v^*, ϕ^*
STEP 5: Correct pressure and velocities
p, u, v, ϕ^*
STEP 6: Solve all other discretised transport equations
ϕ
Convergence?
No
Yes
STOP

This algorithm is implemented in OpenFOAM as follows:

- U equation is defined

```
fvVectorMatrix UEqn
(
            fvm::ddt(U)
          + fvm::div(phi, U)
          - fvm::laplacian(nu, U)
);
```

- The momentum predictor is solved

```
solve (UEqn == -fvc::grad(p));
```

- Calculate the a_p coefficient and calculate U

```
volScalarField rUA = 1.0/UEqn().A();
U = rUA*UEqn().H();
```

- The flux is calculated

```
phi = (fvc::interpolate(U) & mesh.Sf())
+ fvc::ddtPhiCorr(rUA, U, phi);
adjustPhi(phi, U, p);
```

- The pressure equation is defined and solved and this is repeated for the prescribed number of non-orthogonal corrector steps

```
fvScalarMatrix pEqn
(
fvm::laplacian(rUA, p) == fvc::div(phi)
);
pEqn.setReference(pRefCell, pRefValue);
pEqn.solve();
```

- The flux is corrected

```
if (nonOrth == nNonOrthCorr)
{
phi -= pEqn.flux();
}
```

- Continuity errors are calculated

```
# include "continuityErrs.H"
```

- The momentum corrector step is performed

```
U -= rUA*fvc::grad(p);
U.correctBoundaryConditions();
```

2.5.2 Fluid Properties

The flow is incompressible, two-dimensional, laminar and follows Newtonian transport properties, with properties for all the cases given as:

- Density, $\rho = 1$
- Kinematic viscosity, $\nu = \frac{\mu}{\rho}$, which is set to 0.05 in order to obtain Reynolds number $Re = 20$, according to the relation $Re = \frac{Ud}{\nu}$
- Darcy coefficient in the porous region, $D = \frac{1}{K}$, which is set to 1×10^5 in order to obtain Darcy number $Da = 1 \times 10^{-5}$ according to the relation $Da = \frac{K}{d^2}$
- Forchheimer coefficient in the porous region, F is set to zero for the present study

2.5.3 Solution Method and Control

pisoFoam is a transient solver and solves for each time step (until the specified tolerance is obtained) until the end time specified in controlDict is reached. It does not support residual control. Courant number must be less than 1 for a physical solution and pisoFoam terminates the case automatically if Courant number is very large. The time step is suitably reduced such that the Courant number does not increase more than 1. Convergence is observed when the solution does not change with time, i.e. velocity and pressure contours, as well as measurable parameters such as drag coefficient are constant with respect to time.

The fvSolution file defines the solvers used and the desired tolerances in the PISO loop. The same fvSolution file is used for all the cases:

```
solvers
{
    p
    {
        solver          GAMG;
        tolerance       1e-06;
        relTol          0.1;
        smoother        GaussSeidel;
    }

        pFinal
    {
        $p;
        tolerance       1e-06;
        relTol          0;
    }

    "(U|k|epsilon|omega|R|nuTilda).*"
```

```
    {
        solver          smoothSolver;
        smoother        GaussSeidel;
        tolerance       1e-05;
        relTol          0;
    }
    }

    PIMPLE
    {
        nCorrectors     2;
        nNonOrthogonalCorrectors 0;
        pRefCell        0;
        pRefValue       0;
    }
```

GAMG is Geometric agglomerated Algebraic MultiGrid solver used to solve the discretised pressure equation. Discretised velocity equation is solved by smoothSolver. nCorrectors refers to the number of times the pressure correction equation is applied, which is set to 2 to achieve the required tolerance.

The fvSchemes file contains the numerical schemes required to solve various mathematical expressions such as gradient, divergence and laplacian. The same fvSchemes file is used for all the cases:

```
ddtSchemes
{
    default         Euler;
}

gradSchemes
{
    default         Gauss linear;
}

divSchemes
{
    default         none;
    div(phi,U)      Gauss limitedLinearV 1.0;
    div((nuEff*dev2(T(grad(U))))) Gauss linear;
}

laplacianSchemes
{
```

```
    default         Gauss linear corrected;
}

interpolationSchemes
{
    default         linear;
}

snGradSchemes
{
    default         corrected;
}
```

All of the schemes used were chosen for maximum stability, while the 'corrected' parameter was included for laplacianSchemes and snGradSchemes to correct the mesh non-orthogonality, which was maximum approximately 45° for all the cases.

3 Results and Discussions

3.1 Grid Independence Study

Due to the nature of computational methods, in CFD, the accuracy of a solution depends on the mesh fineness. A coarse grid may be computationally economical but not yield solutions of the desired accuracy, meanwhile a fine grid may yield accurate solutions but be computationally costly. Hence, a study needs to be done to determine the required fineness to obtain accurate solutions while keeping the computational cost low. The grids were refined using a grid refinement ratio of approximately 2 until Grid Convergence Index less than 5% was obtained. Richardson Extrapolation was also used to obtain the drag coefficient at zero grid spacing.

3.1.1 Fully Porous Cylinder

Mesh	No. of cells	Coefficient of Drag (C_d)
1	15718	2.148164
2	30400	2.15223
3	61503	2.15622
4	123930	2.158554
Richardson Extrapolation	-	*2.161844*

Table 3: Grid Independence Study for Fully Porous Cylinder

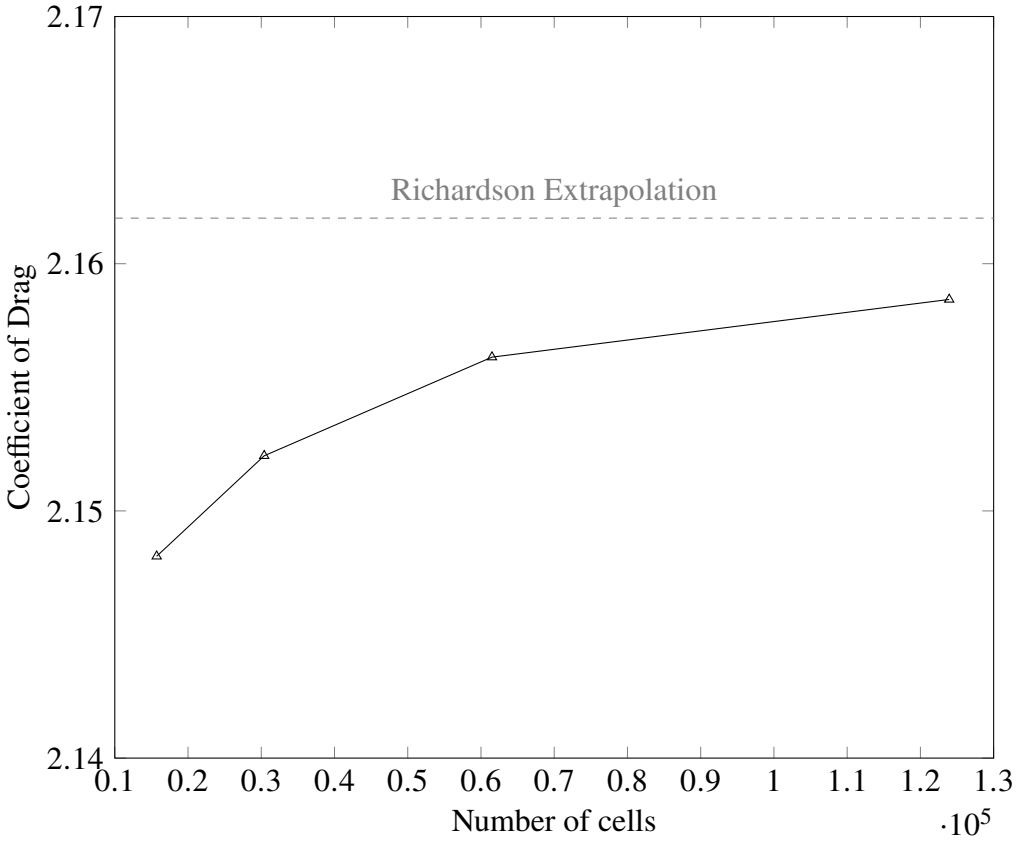

Grid Convergence Indices were obtained as follows:

- GCI_{12} = 12.40%
- GCI_{23} = 0.33%
- GCI_{34} = 0.19%

Hence Mesh 3 was deemed satisfactory to obtain accurate solutions.

3.1.2 Solid Cylinder

Mesh	No. of cells	Coefficient of Drag (C_d)
1	13137	2.171204
2	25600	2.170268
3	51585	2.170176
Richardson Extrapolation	-	*2.170166*

Table 4: Grid Independence Study for Solid Cylinder

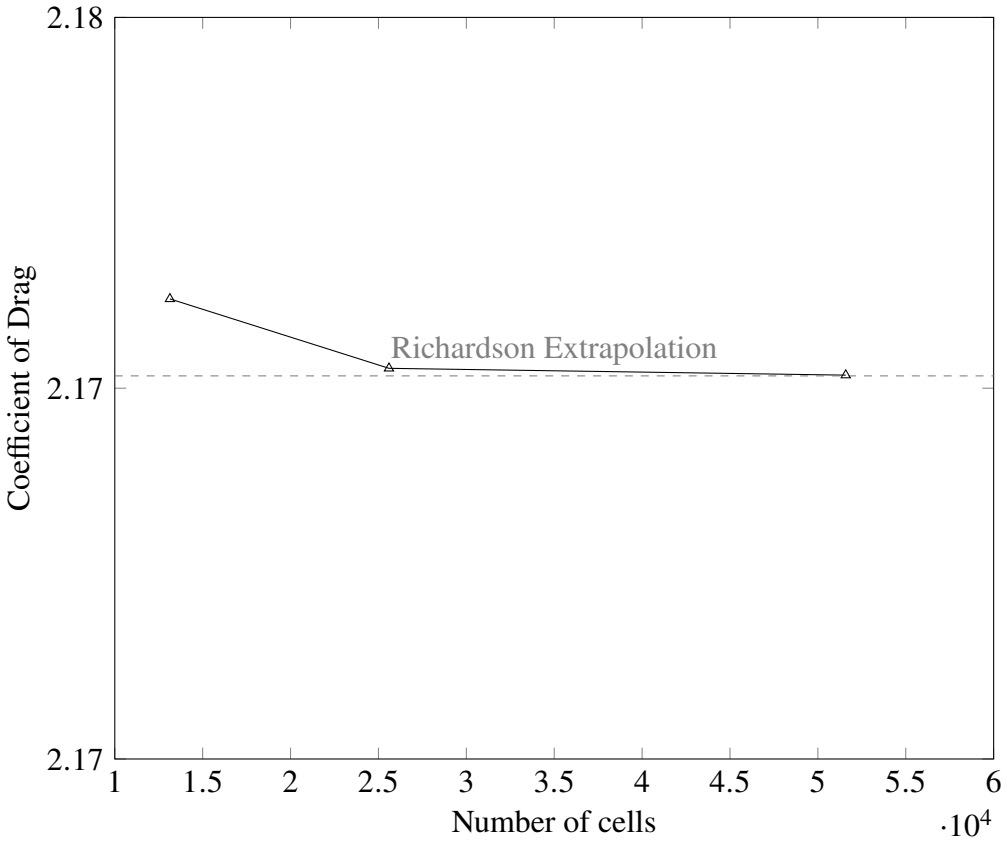

Grid Convergence Indices were obtained as follows:

- $GCI_{12} = 0.005876\%$
- $GCI_{23} = 5.77623 \times 10^{-4}\%$

Hence Mesh 2 was deemed satisfactory to obtain accurate solutions.

3.1.3 Porous Coated Cylinder

Mesh	No. of cells	Coefficient of Drag (C_d)
1	14877	2.146452
2	28800	2.151048
3	58254	2.155504
4	117369	2.158088
Richardson Extrapolation	-	*2.161655*

Table 5: Grid Independence Study for Porous Coated Cylinder

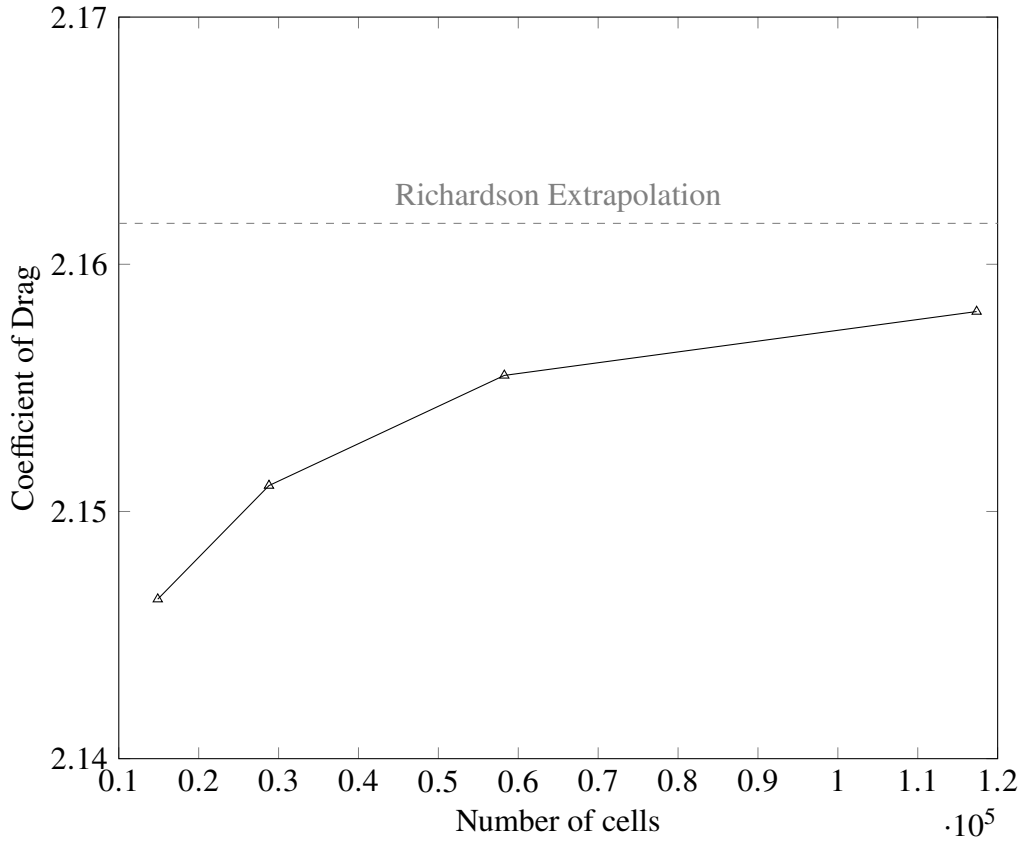

Grid Convergence Indices:

- GCI_{12} = 8.50%
- GCI_{23} = 0.36%
- GCI_{34} = 0.21%

Hence Mesh 3 was deemed satisfactory to obtain accurate solutions.

3.2 Validation

In order to ensure that the results obtained are accurate, the drag coefficient and the wake length for $Re = 20$ and $Da = 1 \times 10^{-5}$ porous cylinder and solid cylinder are compared with those obtained by Yu et al. [2] as shown in Table 6.

Case	**Drag Coefficient, C_d**	**Wake Length, L_f (m)**
Porous Cylinder *(present study)*	2.158554	0.92
Porous Cylinder *(Yu et al. [2])*	1.933	0.902
Solid Cylinder *(present study)*	2.170268	0.88
Solid Cylinder *(Yu et al. [2])*	2.040	0.916

Table 6: Validation

The percentage difference between the results in the present study and the results obtained by Yu et al. [2] are shown in Table 7.

Case	**Percentage difference in C_d**	**Percentage difference in L_f**
Porous Cylinder	11.67%	2.00%
Solid Cylinder	6.38%	3.93%

Table 7: Percentage difference

Hence the results obtained in the present study are in acceptable agreement with the results published by Yu et al. [2]. The degree of error may be attributed to the discretisation schemes used in the present study, as the schemes were selected on the basis of stability and not accuracy. The equation solvers used may also contribute to the error.

3.3 Results

The results of the three cases were studied at $Re = 20$ and $Da = 1 \times 10^{-5}$ by examining the coefficient of drag as well as wake geometry parameters namely wake length, location of recirculating centres, penetration depth and maximum wake width. The wake geometry and the measurement of its parameters are discussed in further detail in Appendix A.

3.3.1 Velocity Contours

It is evident that at this Reynolds number and Darcy number, the velocity contour for porous cases do not differ greatly from that of the solid cylinder, however the fluid can be seen flowing with a small velocity through the porous region.

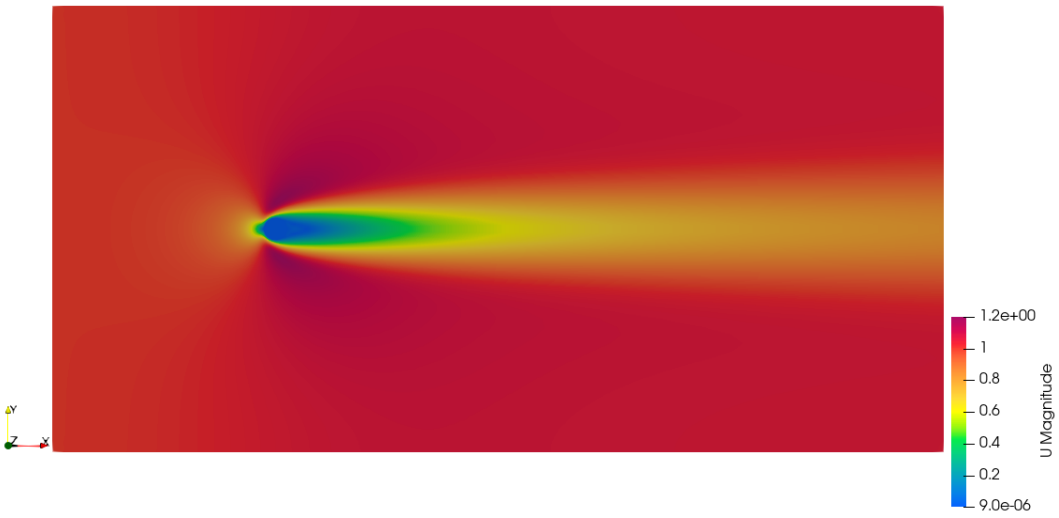

Figure 5: Fully Porous Cylinder

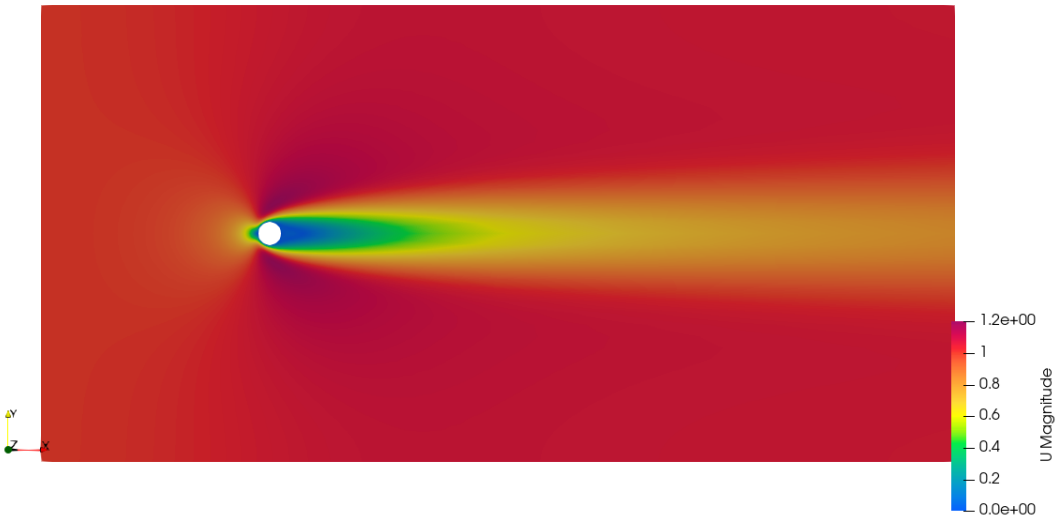

Figure 6: Solid Cylinder

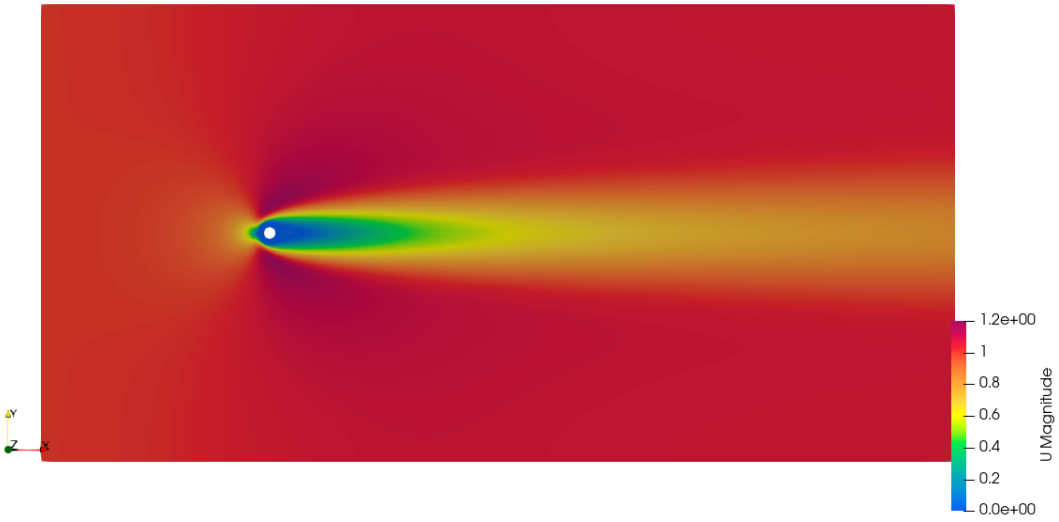

Figure 7: Porous Coated Cylinder

3.3.2 Pressure Contours

The pressure contour for the porous cases show higher maximum pressure (at stagnation point) than solid cylinder case and the porous region affects the pressure distribution near the cylinder significantly.

Figure 8: Fully Porous Cylinder

Figure 9: Solid Cylinder

Figure 10: Porous Coated Cylinder

3.3.3 Streamlines

The streamline pattern for the porous cases shows, as expected, a small amount of fluid passing through the porous region and a modified recirculating wake geometry.

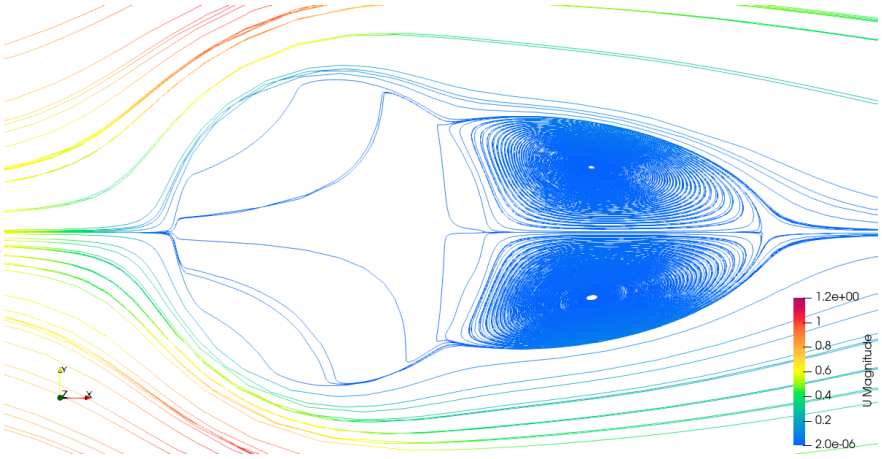

Figure 11: Fully Porous Cylinder

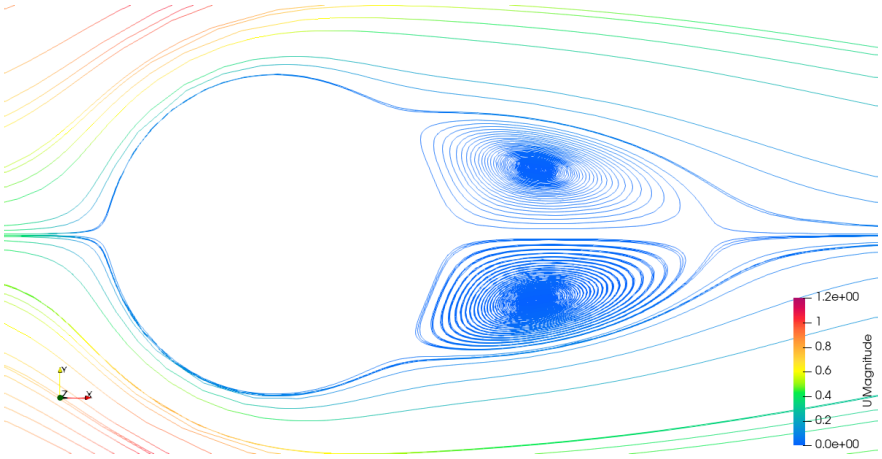

Figure 12: Solid Cylinder

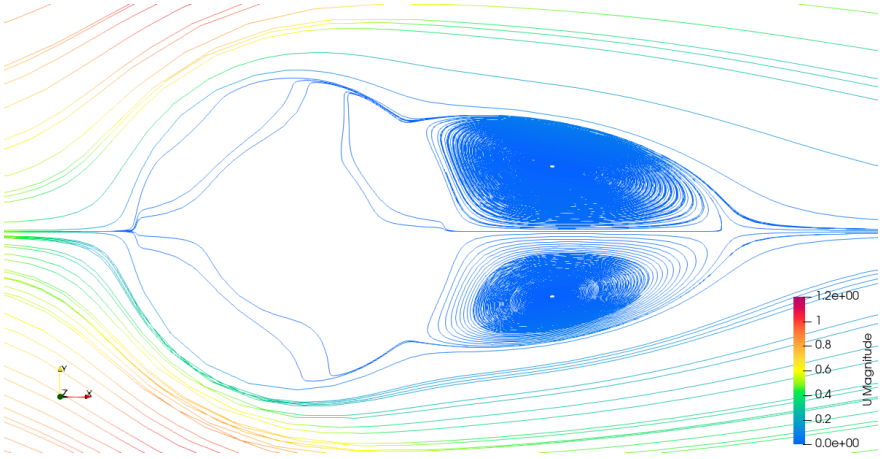

Figure 13: Porous Coated Cylinder

3.4 Comparison

All three cases are compared using drag coefficient (C_d), wake length (L_f), wake center location (a, b), penetration depth (L_p) and maximum wake width (W_e) as shown:

Case	C_d	L_f	a	b	L_p	W_e
Fully Porous Cylinder	2.15622	0.92	0.345	0.42	0.11	0.75
Solid Cylinder	2.170268	0.88	0.36	0.42	-	0.8
Porous Coated Cylinder	2.158088	0.92	0.346	0.42	0.13	0.76

Table 8: Comparison of the cases

It is observed that:

- The value of coefficient of drag of the porous coated cylinder lies between that of the fully porous cylinder and the solid cylinder
- The wake lengths of both porous cylinders are approximately equal and greater than that of the solid cylinder
- The recirculating wake centers are closer to the cylinder in both the porous cases compared to the solid case, which is due to the penetration of the wake into the cylinder
- The maximum wake width of both the porous cylinders is less than that of the solid cylinder

4 Conclusions

The steady dynamics of 2D, laminar flow over porous and porous coated cylinders have been studied and compared with solid cylinder at a Reynolds number $Re = 20$ and Darcy number $Da = 1 \times 10^{-5}$. A Grid Independence Study was performed to obtain mesh-independent results, which are in agreement with previously published results on porous cylinders.

While the present study only investigates the steady dynamics at a particular Re and Da, the case setup is valid for any laminar case as well as unsteady cases, since pisoFoam solver has been used. Different levels of permeability can also be studied by simply changing the Darcy coefficient D according to the desired Darcy number Da. Hence, a larger set of findings at different Reynolds numbers and Darcy numbers can be obtained by simply varying the constant parameters, without actually changing the case setup.

The study of porous cylinders, particularly the reduced drag coefficients and different wake geometries compared to solid cylinders may prove to be of importance in the fields of structural design, aerodynamics, aeroacoustics etc.

5 Acknowledgement

I would like to sincerely thank Prof. Chandan Bose, my project guide, for his consistent support, encouragement, and guidance throughout my project. His wealth of experience and invaluable advice played a pivotal role in helping me successfully accomplish my objectives. I would also like to express my appreciation to Prof Janani Srree Murallidharan for her valuable input and supervision during my internship. My gratitude extends to Mr. Biraj Khadka, my mentor, who had supported and guided me throughout my internship and Ms. Payel Mukherjee, Project Manager of the CFD-OpenFOAM Team at FOSSEE, for their unwavering assistance during my internship. Lastly, I want to thank the entire CFD-OpenFOAM FOSSEE team for offering me this wonderful opportunity. It has been an honour to work with the team, and I am thankful for the knowledge and skills I have acquired during this rewarding journey.

A Wake Geometry

The wake geometry as illustrated in the study on porous cylinders by Yu et al. [2], is shown in Figure 14. The recirculating wakes are visualised in ParaView using the Stream Tracer utility.

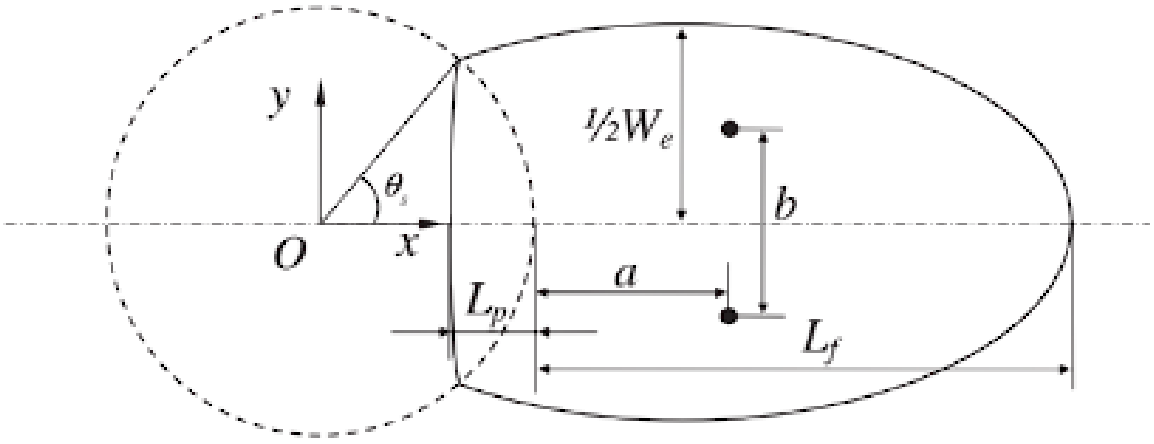

Figure 14: Wake Geometry

A.1 Wake Length (L_f)

The wake length is determined by plotting velocity over the center line and examining the points where velocity crosses zero, as shown in Figure 15.

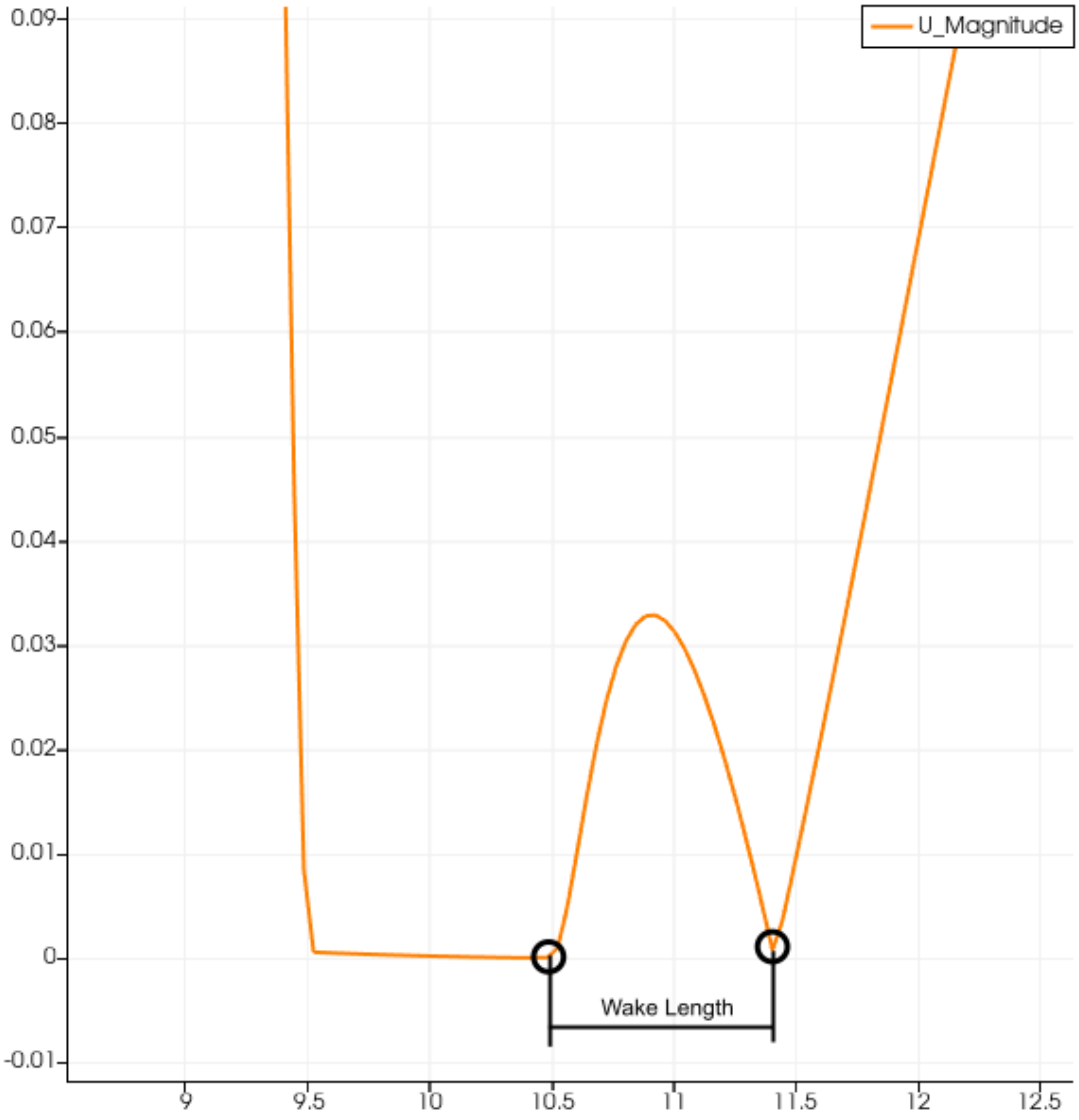

Figure 15: Wake Length

A.2 Location of Recirculating Wake Centres (a, b)

The distances a and b are measured using the ruler tool in ParaView, as shown in Figure 16.

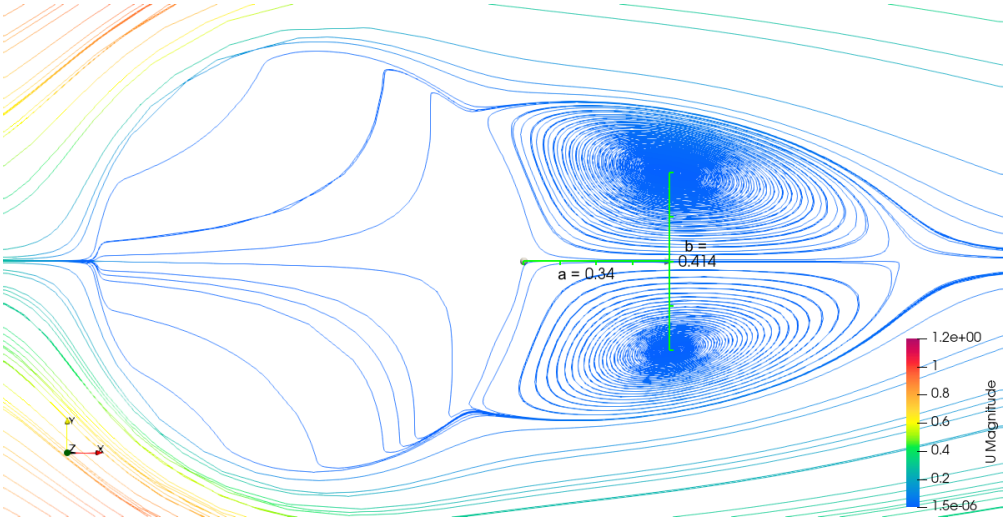

Figure 16: Wake Centers

A.3 Penetration Depth (L_p)

The penetration depth is the distance by which the wake penetrates the porous cylinder and is measured using ruler tool as shown in Figure 17.

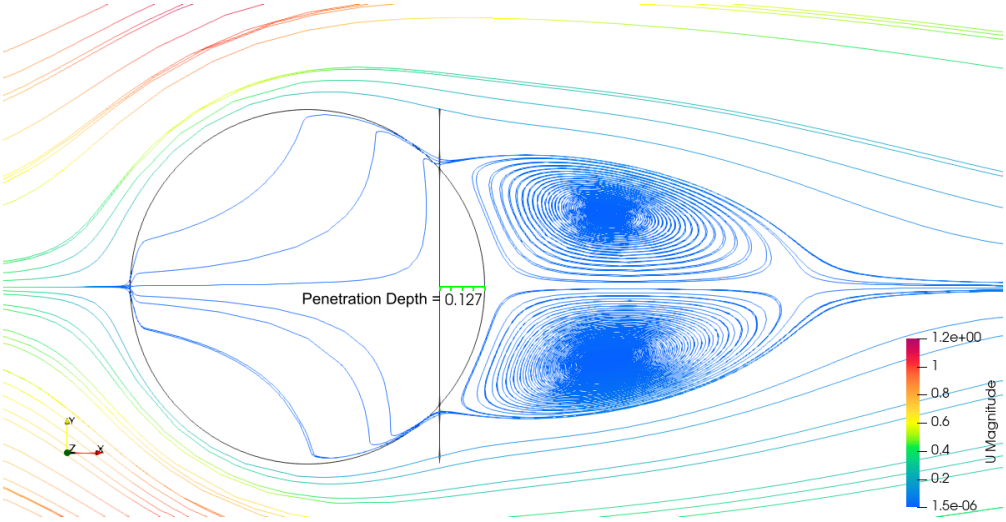

Figure 17: Penetration Depth

A.4 Maximum Wake Width (W_e)

The maximum wake width is measured using the ruler tool in Paraview as shown in Figure 18.

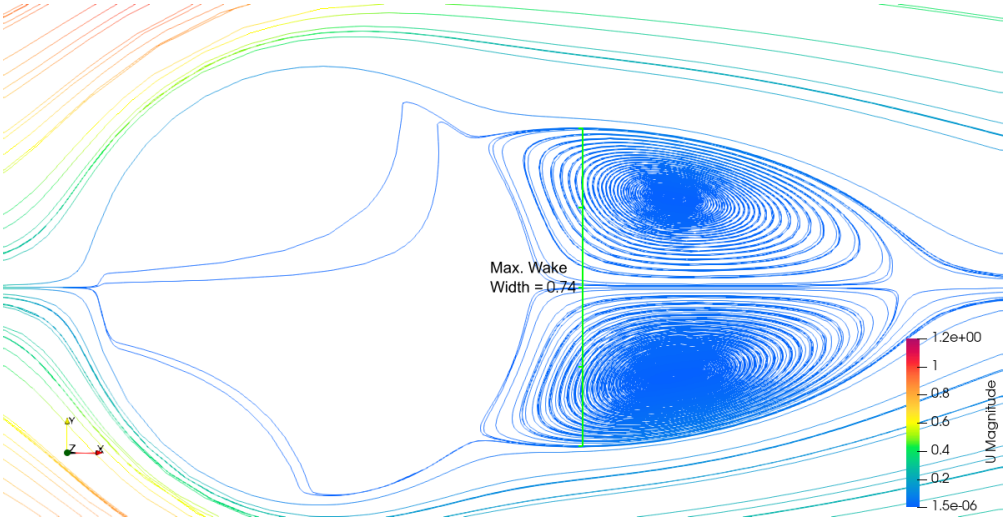

Figure 18: Maximum Wake Width

References

[1] B. Rajani, A. Kandasamy, and S. Majumdar, "Numerical simulation of laminar flow past a circular cylinder," *Applied Mathematical Modelling*, vol. 33, no. 3, pp. 1228–1247, 2009. [Online]. Available: https://www.sciencedirect.com/science/article/pii/S0307904X08000243

[2] P. Yu, Y. Zeng, T. S. Lee, X. B. Chen, and H. T. Low, "Steady flow around and through a permeable circular cylinder," *Computers & Fluids*, vol. 42, no. 1, pp. 1–12, 2011. [Online]. Available: https://www.sciencedirect.com/science/article/pii/S0045793010002690

DISCLAIMER: This project reproduces the results from an existing work, which has been acknowledged in the report. Any query related to the original work should not be directed to the contributor of this project.